Signal Processing 137 (2017) 309–318

Contents lists available at ScienceDirect

Signal Processing

journal homepage: www.elsevier.com/locate/sigpro

Adaptive detection using both the test and training data for disturbance correlation estimation

Jun Liu[a,b], Hong-Yan Zhao[a,b], Weijian Liu[c,*], Hongbin Li[d], Hongwei Liu[a,b]

[a] National Laboratory of Radar Signal Processing, Xidian University, Xi'an 710071, China
[b] Collaborative Innovation Center of Information Sensing and Understanding, Xidian University, Xi'an 710071, China
[c] Wuhan Electronic Information Institute, Wuhan 430019, China
[d] Department of Electrical and Computer Engineering, Stevens Institute of Technology, Hoboken, NJ 07030 USA

ARTICLE INFO

Article history:
Received 22 July 2016
Revised 1 December 2016
Accepted 17 January 2017
Available online 8 February 2017

Keywords:
Adaptive detection
Constant false alarm rate
Mismatched signal rejection
Selectivity
generalized Chi distribution

ABSTRACT

This paper examines a target detection problem in colored Gaussian disturbance with an unknown covariance matrix. In many classic adaptive detectors, the covariance estimator is formed by using only the training data. This necessitates calculating a new covariance estimator for each cell under test (CUT) during the cell-by-cell target search process. We consider herein an alternative approach that forms the covariance matrix estimate by using both test and training data for detection in homogeneous environments. This approach is computationally much more efficient since the covariance matrix estimator is computed only once and can be applied for target detection at each CUT. Using this estimator, we propose a new detector with two tunable parameters, which includes several existing detectors as special cases. Closed-form expressions for the probabilities of false alarm and detection are derived in the matched and mismatched cases for both non-fluctuating and fluctuating target models. Simulation results reveal that the rejection capability of mismatched signals of the proposed detector can be flexibly controlled by adjusting its tunable parameters. In particular, the proposed detector can achieve the same detection performance as the generalized likelihood ratio test (GLRT) detector derived by Kelly, but has a much lower computational burden.

1. Introduction

Target detection in Gaussian disturbance with unknown covariance matrix has been a topic of long-standing interest in radar/sonar signal processing [1–19]. Typically, the presence of target is sought in a (range) cell under test (CUT). The data collected from the CUT is referred to as the test (primary) data. A set of independent and identically distributed training (secondary) data samples, which contain disturbance only, are employed to estimate the unknown disturbance covariance matrix. In radar practice, these training data samples are usually collected from range cells adjacent to the CUT.

Several classic detection algorithms have been proposed in the past. Specifically, Kelly proposed a generalized likelihood ratio test (GLRT) detector through replacing all unknown parameters with their maximum likelihood (ML) estimates under each hypothesis in one step [1]. Meanwhile, an adaptive matched filter (AMF) detector was derived with an *ad hoc* two-step procedure [3]. In particular, it first assumes the disturbance covariance matrix is known and obtains a GLRT by maximizing over other unknown parameters; then a test statistic is obtained by substituting the disturbance covariance matrix with its ML estimate based on the training data alone. In [4], an adaptive coherence estimator (ACE) was proposed to handle a non-homogeneity between the test and training data. A prominent feature of the above three detectors is that they all achieve constant false alarm rate (CFAR) with respect to the unknown disturbance covariance matrix. Note that the performance of the GLRT, AMF and ACE cannot be flexibly adjusted. In the last two decades, researchers have proposed many tunable detectors including parametric [10] and two-stage receivers [20–23].

Since the location of the target to be detected is generally unknown in practice, a grid search is often resorted to, which divides the desired radar surveillance area into many (range) cells or bins. We need to test each cell one by one to decide whether the interested target is present or not. For target detection in a specific cell, a standard approach is to employ the data collected from cells adjacent to the CUT as training data, and then use these training

* Corresponding author.
E-mail addresses: junliu@xidian.edu.cn (J. Liu), zhaohongyan@stu.xidian.edu.cn (H.-Y. Zhao), liuvjian@163.com (W. Liu), hongbin.li@stevens.edu (H. Li), hwliu@xidian.edu.cn (H. Liu).

http://dx.doi.org/10.1016/j.sigpro.2017.01.017
0165-1684/

data to estimate the disturbance covariance matrix. Obviously, the training data are different for different CUTs, which implies that a new estimate of the disturbance covariance matrix has to be calculated for a distinct CUT in the detectors mentioned above. This operation entails heavy computational complexity, particularly in space-time adaptive processing [24,25], where the data dimension is the product of the number of array elements and the number of taps of the Doppler filters which can be quite high even with a moderate number of array antennas and filter taps.

For target detection in homogeneous environments, Gerlach in [26] introduced a new covariance matrix estimator to avoid calculating a large number of covariance matrices and their inverses by employing both the test and training data. Note that the idea of using the whole data block for estimation is similar to the mean level adaptive detector (MLAD) with scalar data [27,28]. Once the disturbance covariance matrix estimate is calculated with the whole data block, it can be applied for detection in each cell. Apparently, this approach is computationally much more efficient. It should be pointed out that the whole data might contain a target signal, which can lead to some performance loss, but at the benefit of significantly reducing the computational complexity. The performance loss is considered negligible when the training size is sufficiently large and targets are rare.

Based on the covariance estimator using both the test and training data, we propose in this paper a new detector with two tunable parameters a and b, which includes the detector in [26] as a special case. In particular, the proposed detector with $a = 1$ and $b = -1$ provides the same detection performance as Kelly's GLRT detector. It should be emphasized that the proposed detector has a much lower computational burden than the conventional detectors (i.e., Kelly's GLRT, the AMF, and the ACE). The statistical properties of the proposed detector are investigated for both the matched and mismatched cases depending on whether the actual steering vector is aligned with the nominal one. It should be pointed out that the mismatched case is not studied in [26]. Closed-form expressions for the probabilities of false alarm and detection of the proposed detector are derived for both non-fluctuating and fluctuating target models. In the non-fluctuating model, the target amplitude is considered to be deterministic, while in the fluctuating model, the target amplitude is assumed to have a generalized Chi distribution which includes the Rayleigh distribution as a special case. These theoretical results are confirmed by using Monte Carlo (MC) simulations. Numerical results demonstrate that the selective capability of the proposed detector can be flexibly adjusted by changing the tunable parameters.

The remainder of this paper is organized as follows. Section 2 formulates the problem to be studied. In Section 3, a detector with tunable parameters is proposed, and performance analysis is provided in detail. Simulation results are illustrated in Section 4 and finally the paper is summarized in Section 5.

Notation. Vectors (matrices) are denoted by boldface lower (upper) case letters. Superscripts $(\cdot)^T$, $(\cdot)^*$ and $(\cdot)^\dagger$ denote transpose, complex conjugate and complex conjugate transpose, respectively. The notation $\sim$ means "is distributed as," and $\mathcal{CN}$ denotes a circularly symmetric, complex Gaussian distribution. $\overset{\mathrm{d}}{=}$ means the former and latter random quantities have the same distribution. χ^2_n denotes a real central Chi-squared distribution with n degrees of freedom, while $\chi'^2_n(\zeta)$ denotes a real non-central Chi-squared distribution with n degrees of freedom and a non-centrality parameter ζ. $|\cdot|$ represents the modulus of a complex number and $\jmath = \sqrt{-1}$. $\mathrm{C}_n^m = \frac{n!}{m!(n-m)!}$ and $\Gamma(\cdot)$ are the binomial coefficient and the Gamma function, respectively.

2. Data model

Consider the following model of the received data in a CUT:

$$\mathbf{x} = \alpha\,\mathbf{s} + \mathbf{n}, \tag{1}$$

where $\mathbf{s}$ is a known steering vector of dimension $N \times 1$; α is a deterministic but unknown complex scalar accounting for the target reflectivity and the channel propagation effects; the disturbance $\mathbf{n}$ is assumed to have a circularly symmetric, complex Gaussian distribution, i.e., $\mathbf{n} \sim \mathcal{CN}(\mathbf{0}, \mathbf{R})$, where $\mathbf{R}$ is a positive definite covariance matrix of dimension $N \times N$. These data may be temporal samples, spatial samples (obtained with an array), or any mix of the above.

In practice, the disturbance covariance matrix $\mathbf{R}$ is usually unknown. To estimate it, we impose a standard assumption that there exists a set of homogeneous secondary data free of target signal components, i.e., $\{\mathbf{y}_k | \mathbf{y}_k \sim \mathcal{CN}(\mathbf{0}, \mathbf{R}), k = 1, 2, \ldots, K \text{ and } K \geq N\}$. In array signal processing, this set of secondary data are usually collected from the range cells adjacent to the CUT. Let the null hypothesis (H_0) be that the target signal is free in the test data and the alternative hypothesis (H_1) be that the test data contain the target signal. Hence, the detection problem is to decide between the null hypothesis

$$H_0 : \begin{cases} \mathbf{x} \sim \mathcal{CN}(\mathbf{0},\ \mathbf{R}) \\ \mathbf{y}_k \sim \mathcal{CN}(\mathbf{0},\ \mathbf{R}),\ \ k = 1, \ldots, K, \end{cases} \tag{2a}$$

and the alternative one

$$H_1 : \begin{cases} \mathbf{x} \sim \mathcal{CN}(\alpha\mathbf{s},\ \mathbf{R}) \\ \mathbf{y}_k \sim \mathcal{CN}(\mathbf{0},\ \mathbf{R}),\ \ k = 1, \ldots, K. \end{cases} \tag{2b}$$

It is easy to show that based on these secondary data, the ML estimate of the disturbance covariance matrix (up to a scaling factor) is

$$\hat{\mathbf{R}} = \sum_{k=1}^{K} \mathbf{y}_k \mathbf{y}_k^\dagger. \tag{3}$$

Using this disturbance covariance matrix estimate, several classic adaptive detectors were proposed, including, e.g., the GLRT [1], AMF [3], and ACE [4]:

$$T_{\mathrm{GLRT}} = \frac{|\mathbf{s}^\dagger \hat{\mathbf{R}}^{-1}\mathbf{x}|^2}{(\mathbf{s}^\dagger \hat{\mathbf{R}}^{-1}\mathbf{s})(1 + \mathbf{x}^\dagger \hat{\mathbf{R}}^{-1}\mathbf{x})} \underset{H_0}{\overset{H_1}{\gtrless}} t_{\mathrm{GLRT}}, \tag{4}$$

$$T_{\mathrm{AMF}} = \frac{|\mathbf{s}^\dagger \hat{\mathbf{R}}^{-1}\mathbf{x}|^2}{\mathbf{s}^\dagger \hat{\mathbf{R}}^{-1}\mathbf{s}} \underset{H_0}{\overset{H_1}{\gtrless}} t_{\mathrm{AMF}}, \tag{5}$$

$$T_{\mathrm{ACE}} = \frac{|\mathbf{s}^\dagger \hat{\mathbf{R}}^{-1}\mathbf{x}|^2}{(\mathbf{s}^\dagger \hat{\mathbf{R}}^{-1}\mathbf{s})(\mathbf{x}^\dagger \hat{\mathbf{R}}^{-1}\mathbf{x})} \underset{H_0}{\overset{H_1}{\gtrless}} t_{\mathrm{ACE}}. \tag{6}$$

In the applications of the above three detectors, we need to calculate a new covariance estimator for a different CUT in the grid search stage, which incurs heavy computational burdens, especially when the data dimension is high (e.g., in space-time adaptive processing [24,25]), and/or the number of cells to be tested is large (e.g., in high-resolution radar).

3. Detector with tunable parameters

To alleviate the computational burden stated above, we estimate the disturbance covariance matrix by using both the test and training data, i.e.,

$$\tilde{\mathbf{R}} = \hat{\mathbf{R}} + \mathbf{x}\mathbf{x}^\dagger. \tag{7}$$

Using this estimator, we propose a new detector with two tunable parameters as follows

$$\Lambda = \frac{|\mathbf{s}^\dagger \tilde{\mathbf{R}}^{-1}\mathbf{x}|^2}{(\mathbf{s}^\dagger \tilde{\mathbf{R}}^{-1}\mathbf{s})(a + b\,\mathbf{x}^\dagger \tilde{\mathbf{R}}^{-1}\mathbf{x})} \underset{H_0}{\overset{H_1}{\gtrless}} \lambda, \tag{8}$$

where λ denotes a detection threshold, a and b are tunable parameters.

Note that the whole data block including both the test and training data are used to calculate the disturbance covariance matrix estimate. Signal contamination affects the accuracy of the disturbance covariance matrix estimate through $\tilde{\mathbf{R}}$ in (7). If multiple targets appear in the training data, the accuracy of the disturbance covariance matrix estimate is likely to be further reduced, and so is the detection performance of the proposed detector. Nevertheless, the performance loss is small when the training size is large and targets are rare.

It should be emphasized that the proposed detector using $\tilde{\mathbf{R}}$ in (7) instead of $\hat{\mathbf{R}}$ in (3) has the benefit of lower computational burden. Assume that the total number of cells under test in the grid search is M which is usually much larger than N, i.e., $M \gg N$. The dominant complexity in the classical detectors (4)–(6) or the proposed detector (8) is the matrix inversion. The complexity of the proposed detector is $\mathcal{O}(N^3)$ flops, because that once the estimate $\tilde{\mathbf{R}}$ in (7) is obtained, we can use it for target detection in all CUTs during the stage of grid search. In contrast, the complexity of the classical detectors (4)–(6) is $\mathcal{O}(MN^3)$ flops, due to the requirement of calculating a different estimate of the disturbance covariance matrix for each CUT in the grid search.

Note that the two parameters a and b in (8) cannot be simultaneously zero, and $a \geq 0$. Since scaling the test statistic gives an equivalent one in the sense that the detection performance is the same, the term $(a + b\,\mathbf{x}^\dagger \tilde{\mathbf{R}}^{-1}\mathbf{x})$ in the denominator of the test statistic Λ in (8) can be equivalently transformed as $(1 + \frac{b}{a}\,\mathbf{x}^\dagger \tilde{\mathbf{R}}^{-1}\mathbf{x})$ by scaling $\frac{1}{a}$ (if $a \neq 0$). Nevertheless, we keep both parameters in (8) so that two special cases of interest are included: 1) $a = 0$ and $b \neq 0$; 2) $a \neq 0$ and $b = 0$. The detector in (8) is very general, which includes several existing detectors as special cases.

- For $a = 1$ and $b = -1$, it has the same detection performance as Kelly's GLRT detector[1] [1]; however, the proposed detector (8) in this case has a form different from Kelly's GLRT detector, and is computationally simpler to implement, since the former just needs to calculate one covariance matrix and its inverse in the grid search stage, while the latter has to calculate a new covariance matrix and its inverse for a distinct CUT;
- For $a = 1$ and $b = 1$, it corresponds to Kelly's GLRT with $\hat{\mathbf{R}}$ replaced by the new covariance matrix estimator $\tilde{\mathbf{R}}$;
- For $a = 1$ and $b = 0$, it is the Rao test in [8];
- For $a = 0$ and $b = 1$, it is the ACE with $\hat{\mathbf{R}}$ replaced by $\tilde{\mathbf{R}}$.

In some practical scenarios, the true target steering vector $\mathbf{s}_0$ may not be aligned with the nominal one $\mathbf{s}$, due to many factors such as array calibration and/or position errors, imperfect antenna shape, and wavefront distortions. Denote by ϕ the angle between the actual and nominal steering vectors, i.e.,

$$\cos^2\phi = \frac{|\mathbf{s}_0^\dagger \mathbf{R}^{-1}\mathbf{s}|^2}{(\mathbf{s}^\dagger \mathbf{R}^{-1}\mathbf{s})(\mathbf{s}_0^\dagger \mathbf{R}^{-1}\mathbf{s}_0)}. \tag{9}$$

In the following, we investigate the statistical properties of the proposed detector in both the matched ($\phi = 0$) and mismatched ($\phi \neq 0$) cases, and then derive closed-form expressions for its probabilities of false alarm and detection in non-fluctuating and fluctuating target models.

Define

$$\bar{T}_{\mathrm{GLRT}} = \frac{T_{\mathrm{GLRT}}}{1 - T_{\mathrm{GLRT}}} \tag{10}$$

and

$$\rho = \frac{T_{\mathrm{GLRT}}}{T_{\mathrm{AMF}}(1 - T_{\mathrm{GLRT}})}, \tag{11}$$

where T_{GLRT} and T_{AMF} are given in (4) and (5), respectively. As shown in Appendix A, the proposed tunable detector in (8) can be equivalently written as

$$\bar{T}_{\mathrm{GLRT}} \underset{H_0}{\overset{H_1}{\gtrless}} \xi, \tag{12}$$

where

$$\xi = \frac{\lambda(a + b) - b\rho\lambda}{\rho - \lambda(a + b)}. \tag{13}$$

3.1. Non-fluctuating target model

First, we consider the non-fluctuating model where the target amplitude α is deterministic. According to [29], the distribution of $\bar{T}_{\mathrm{GLRT}}$ conditioned on ρ can be expressed as

$$\bar{T}_{\mathrm{GLRT}} \overset{\mathrm{d}}{=} \begin{cases} \frac{\chi_2^2}{\chi^2_{2(K-N+1)}}, & \text{under } H_0 \\ \frac{\chi'^2_2(2\delta\rho)}{\chi^2_{2(K-N+1)}}, & \text{under } H_1 \end{cases} \tag{14}$$

where

$$\delta = |\alpha|^2 \mathbf{s}_0^\dagger \mathbf{R}^{-1}\mathbf{s}_0 \cos^2\phi. \tag{15}$$

Moreover, the PDF of ρ is [29]

$$p_\rho(\rho) = \exp(-\rho\Omega_\phi) \sum_{n=0}^{K-N+2} \mathrm{C}^n_{K-N+2} \frac{K!}{(K+n)!} \times \Omega_\phi^n f_{K-N+2,N+n-1}(\rho), \tag{16}$$

where

$$\Omega_\phi = |\alpha|^2 \mathbf{s}_0^\dagger \mathbf{R}^{-1}\mathbf{s}_0 \sin^2\phi, \tag{17}$$

and

$$f_{k,m}(x) = \frac{(k+m-1)!}{(k-1)!(m-1)!} x^{k-1}(1-x)^{m-1} \tag{18}$$

with $0 < x < 1$. Under H_0, we have $\Omega_\phi = 0$. Then, the PDF of ρ reduces to

$$p_\rho(\rho) = \frac{K!}{(K-N+1)!(N-2)!} \rho^{K-N+1}(1-\rho)^{N-2}. \tag{19}$$

Similar to the derivation in [30], the probability of false alarm can be obtained as

$$P_{\mathrm{FA}} = \int_{(a+b)\lambda}^1 P_{\mathrm{FA}|\rho}\, p_\rho(\rho)\mathrm{d}\rho, \tag{20}$$

where $p_\rho(\rho)$ is given in (19), and

$$P_{\mathrm{FA}|\rho} = \left[\frac{\rho(1 - b\lambda)}{\rho - (a+b)\lambda}\right]^{-(K-N+1)}. \tag{21}$$

Substituting (19) and (21) into (20) yields

$$P_{\mathrm{FA}} = \frac{K!(1 - b\lambda)^{-(K-N+1)}}{(K-N+1)!(N-2)!} J, \tag{22}$$

[1] As derived in (45) of Appendix A, the proposed detector (8) with $a = 1$ and $b = -1$ can be rewritten as $\Lambda = \frac{T_{\mathrm{GLRT}}}{1 - T_{\mathrm{GLRT}}}$. It is known that any monotonic transformation on the statistic test does not change the detection performance. Hence, the proposed detector (8) with $a = 1$ and $b = -1$ is equivalent to Kelly's GLRT detector in terms of detection performance.

where

$$J=\int_{(a+b)\lambda}^{1}(1-\rho)^{N-2}[\rho-(a+b)\lambda]^{K-N+1}\mathrm{d}\rho. \tag{23}$$

According to [31, Eq. (3.196.3)], we obtain

$$J=[1-(a+b)\lambda]^{K}\frac{(K-N+1)!(N-2)!}{K!}. \tag{24}$$

Substituting (24) into (22) results in

$$P_{\mathrm{FA}}=\frac{[1-(a+b)\lambda]^{K}}{(1-b\lambda)^{K-N+1}}. \tag{25}$$

It is obvious that the probability of false alarm is not related to the disturbance covariance matrix. Hence, the proposed detector has the CFAR property with respect to the disturbance covariance matrix. Furthermore, the detection probability of the proposed detector can be calculated by

$$P_{\mathrm{D}}=\int_{(a+b)\lambda}^{1}P_{\mathrm{D}|\rho}p_{\rho}(\rho)\mathrm{d}\rho, \tag{26}$$

where $p_{\rho}(\rho)$ is given in (16), and

$$\begin{aligned}P_{\mathrm{D}|\rho}=&1-\left[\frac{\rho(1-b\lambda)}{\rho-\lambda(a+b)}\right]^{-(K-N+1)}\sum_{j=1}^{K-N+1}\mathrm{C}_{K-N+1}^{j}\\&\times\left[\frac{\lambda(a+b)-b\rho\lambda}{\rho-\lambda(a+b)}\right]^{j}\exp\left[-\frac{\delta\rho-\delta\lambda(a+b)}{1-b\lambda}\right]\\&\times\sum_{m=0}^{j-1}\frac{1}{m!}\left[\frac{\delta\rho-\delta\lambda(a+b)}{1-b\lambda}\right]^{m}.\end{aligned} \tag{27}$$

Note that (27) is obtained in a way similar to that in [30, Eq. 15].

3.2. Fluctuating target model

In the above analysis we assume that the amplitude α is deterministic. However, in many practical scenarios α may be better described with a fluctuating model where α is random [32]. Therefore, it is of interest to examine how the proposed detector performs with the fluctuating target model.

Let $\alpha=|\alpha|\exp(\jmath\theta)$. The phase θ is often assumed to be uniformly distributed within the interval $[0,\ 2\pi)$, while many distributions have been used to describe the statistical characterization of the amplitude $|\alpha|$. We consider that $|\alpha|$ has a generalized Chi distribution [33–35], namely, the PDF of $|\alpha|$ is

$$p_{|\alpha|}(x)=\frac{2\,Q^{Q}x^{2Q-1}}{\sigma_{\alpha}^{2Q}\Gamma(Q)}\exp\left(-\frac{Qx^{2}}{\sigma_{\alpha}^{2}}\right),\quad x>0, \tag{28}$$

where the scale parameter Q controls the fluctuation span, and σ_{α}^{2} denotes the target power. Note that the above generalized Chi distribution in (28) includes the Rayleigh distribution as a spacial case with $Q=1$. In this special case, α is a complex Gaussian variable, i.e., $\alpha\sim\mathcal{CN}(0,\sigma_{\alpha}^{2})$.

Define

$$r=\sigma_{\alpha}^{-2}|\alpha|^{2}, \tag{29}$$

$$\bar{\Omega}_{\phi}=\sigma_{\alpha}^{2}\mathbf{s}_{0}^{\dagger}\mathbf{R}^{-1}\mathbf{s}_{0}\sin^{2}\phi, \tag{30}$$

and

$$\bar{\delta}=\sigma_{\alpha}^{2}\mathbf{s}_{0}^{\dagger}\mathbf{R}^{-1}\mathbf{s}_{0}\cos^{2}\phi, \tag{31}$$

Then, we have

$$\Omega_{\phi}=r\bar{\Omega}_{\phi}\quad\text{and}\quad\delta=r\bar{\delta}. \tag{32}$$

From (28) and (29) we can derive the PDF of r as

$$p_{r}(r)=\frac{Q^{Q}r^{Q-1}}{\Gamma(Q)}\exp(-Qr),\quad r>0. \tag{33}$$

Therefore, the detection probability of the proposed detector in the fluctuating model can be expressed as

$$P_{\mathrm{D}}=\int_{(a+b)\lambda}^{1}\underbrace{\int_{0}^{+\infty}P_{\mathrm{D}|\rho}p_{\rho}(\rho)p_{r}(r)\mathrm{d}r}_{W_{\rho}}\mathrm{d}\rho. \tag{34}$$

Taking (16), (27), (32) and (33) into W_{ρ} defined in (34), and after some algebra, we obtain

$$W_{\rho}=W_{1}-W_{2}, \tag{35}$$

where

$$\begin{aligned}W_{1}=&\frac{K!Q^{Q}}{\Gamma(Q)}\sum_{n=0}^{K-N+2}\frac{\mathrm{C}_{K-N+2}^{n}\bar{\Omega}_{\phi}^{n}}{(K+n)!}f_{K-N+2,N+n-1}(\rho)\\&\times\int_{0}^{+\infty}\exp[-(\rho\bar{\Omega}_{\phi}+Q)r]r^{n+Q-1}\mathrm{d}r\\=&\frac{K!Q^{Q}}{\Gamma(Q)}\sum_{n=0}^{K-N+2}\mathrm{C}_{K-N+2}^{n}\frac{\Gamma(n+Q)}{(K+n)!}\bar{\Omega}_{\phi}^{n}\\&\times(Q+\rho\bar{\Omega}_{\phi})^{-(n+Q)}f_{K-N+2,N+n-1}(\rho)\end{aligned} \tag{36}$$

with $\bar{\Omega}_{\phi}$ defined in (30), and the second equation obtained from [31, eq. (3.351.3)], and

$$\begin{aligned}W_{2}=&\frac{K!Q^{Q}}{\Gamma(Q)}\left[\frac{\rho(1-b\lambda)}{\rho-\lambda(a+b)}\right]^{-(K-N+1)}\sum_{j=1}^{K-N+1}\mathrm{C}_{K-N+1}^{j}\\&\times\left[\frac{\lambda(a+b)-b\rho\lambda}{\rho-\lambda(a+b)}\right]^{j}\sum_{m=0}^{j-1}\frac{1}{m!}\left[\frac{\bar{\delta}\rho-\bar{\delta}\lambda(a+b)}{1-b\lambda}\right]^{m}\\&\times\sum_{n=0}^{K-N+2}\frac{\mathrm{C}_{K-N+2}^{n}\bar{\Omega}_{\phi}^{n}}{(K+n)!}f_{K-N+2,N+n-1}(\rho)\\&\times\int_{0}^{+\infty}r^{n+Q+m-1}\exp\left[-\left(Q+\rho\bar{\Omega}_{\phi}+\frac{\bar{\delta}\rho-\bar{\delta}\lambda(a+b)}{1-b\lambda}\right)r\right]\mathrm{d}r\\=&\frac{K!Q^{Q}}{\Gamma(Q)}\left[\frac{\rho(1-b\lambda)}{\rho-\lambda(a+b)}\right]^{-(K-N+1)}\sum_{j=1}^{K-N+1}\mathrm{C}_{K-N+1}^{j}\\&\times\left[\frac{\lambda(a+b)-b\rho\lambda}{\rho-\lambda(a+b)}\right]^{j}\sum_{m=0}^{j-1}\frac{1}{m!}\left[\frac{\bar{\delta}\rho-\bar{\delta}\lambda(a+b)}{1-b\lambda}\right]^{m}\\&\times\sum_{n=0}^{K-N+2}\mathrm{C}_{K-N+2}^{n}\frac{\Gamma(m+n+Q)}{(K+n)!}\bar{\Omega}_{\phi}^{n}\\&\times\left[Q+\rho\bar{\Omega}_{\phi}+\frac{\bar{\delta}\rho-\bar{\delta}\lambda(a+b)}{1-b\lambda}\right]^{-(m+n+Q)}\\&\times f_{K-N+2,N+n-1}(\rho),\end{aligned} \tag{37}$$

with $\bar{\delta}$ defined in (31), and the second equation obtained from [31, Eq. (3.351.3)]. Applying (35) to (34), we obtain a one-dimensional integral expression for the detection probability of the proposed detector in the fluctuating model.

4. Numerical results

In this section, numerical simulations are conducted to confirm the validity of the above theoretical results. A uniform linear array of $N=8$ elements with a half-wavelength spacing is used. The

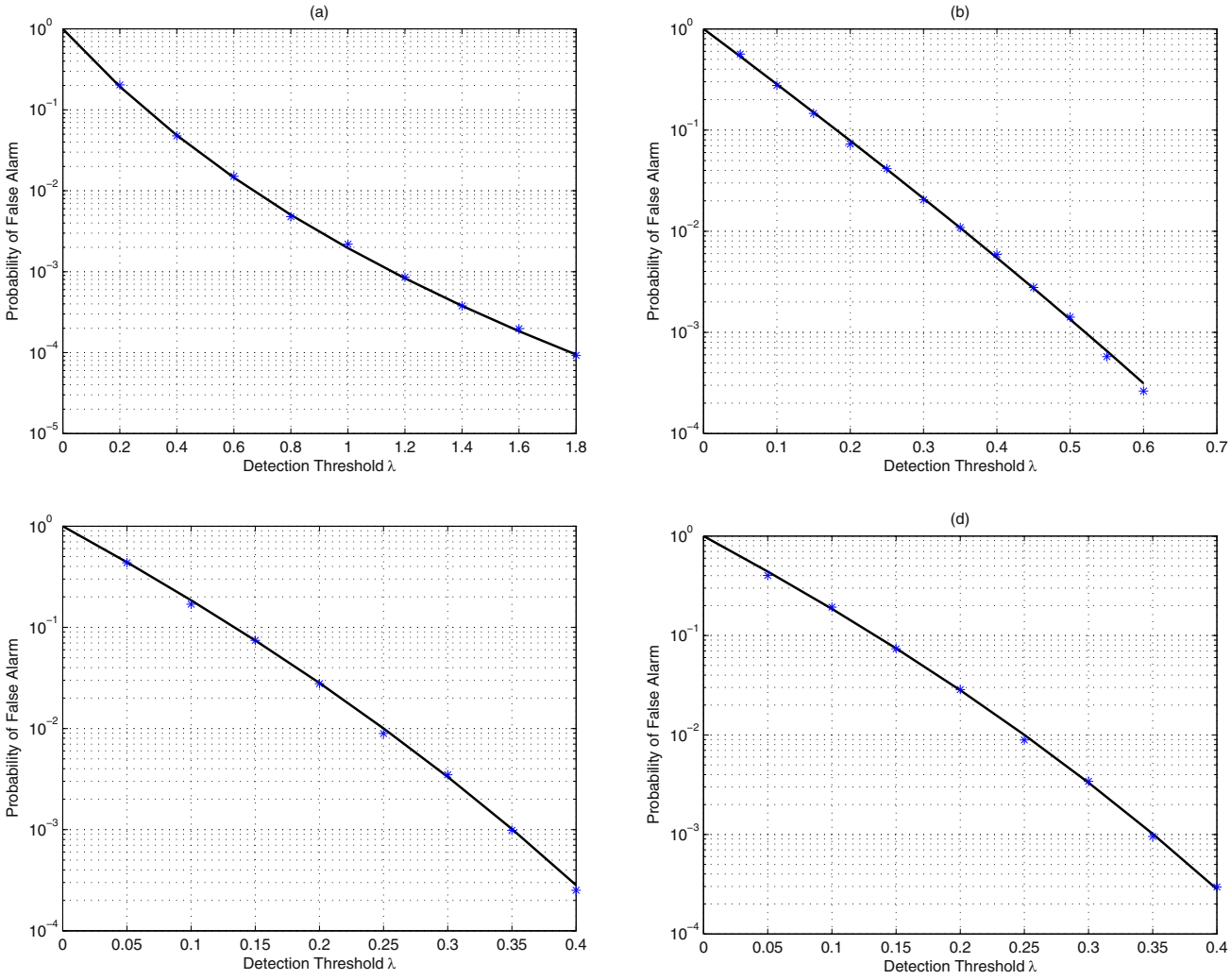

Fig. 1. Probability of false alarm versus the detection threshold for $K = 16$. The lines denote the results obtained with the theoretical expression (25), while the symbols denote the MC results. (a) $b = -1$; (b) $b = -0.5$; (c) $b = 0$; (d) $b = 1$.

probability of false alarm is set to be 10^{-3}. The nominal steering vector is supposed to be

$$\mathbf{s}(\theta) = \frac{1}{\sqrt{N}}\left[1, \cdots, \exp\left(-\jmath\,\pi\,(N-1)\sin\left(\frac{\theta\,\pi}{180}\right)\right)\right]^T \tag{38}$$

with $\theta = 10^\circ$. Assume that the actual signal comes from the angle of θ_0, namely, the actual steering vector is $\mathbf{s}(\theta_0)$. Define the angle mismatch by

$$\Delta\theta = \theta_0 - \theta. \tag{39}$$

When $\Delta\theta = 0^\circ$, the nominal steering vector is aligned with the actual one, while $\Delta\theta \neq 0^\circ$ corresponds to the case of mismatch in the steering vector.

Suppose that the disturbance consists of three jammers and thermal noise, and the jammers come from the angles $\theta_1 = -40^\circ$, $\theta_2 = -10^\circ$ and $\theta_3 = 20^\circ$. The disturbance covariance matrix can be written as

$$\mathbf{R} = \sum_{k=1}^{3}\sigma_k^2\mathbf{s}(\theta_k)\mathbf{s}^\dagger(\theta_k) + \sigma_{\mathrm{n}}^2\mathbf{I}, \tag{40}$$

where σ_k^2 and σ_{n}^2 are the jammer power and thermal disturbance power, respectively, and $\mathbf{I}$ is the identity matrix. In the following simulations, we assume the interference-to-noise ratio (INR) is 30 dB for each jammer.

Unless otherwise specified, we fix $a = 1$ in the following simulations. The parameter b is adjusted to obtain different detectors. It is shown in (44) that $0 < \mathbf{x}^\dagger\tilde{\mathbf{R}}^{-1}\mathbf{x} < 1$. When a is chosen to be 1, the value of b has to be no less than -1 (i.e., $b \geq -1$) to ensure the positiveness of the detection statistic Λ.

Fig. 1 plots the probability of false alarm with respect to the threshold for different values of the tunable parameter b. Here, we select $K = 2N = 16$. The line represents the results obtained with (25), while the symbol denotes the results obtained using MC simulation techniques. The number of independent trials used in each case is $100/P_{\mathrm{FA}}$. It can be seen that the theoretical results match the MC results pretty well.

In Fig. 2, the detection performance of the proposed detector versus the tunable parameter b is presented for both matched and mismatched cases in the non-fluctuating target model. Define the signal-to-noise ratio (SNR) as $\mathrm{SNR} = 10\log_{10}\frac{|\alpha|^2}{\sigma_{\mathrm{n}}^2}$. Here, we choose $K = 16$ and SNR $= 0$ dB. The line represents the results obtained with (26), while the symbol denotes the MC results. The number of independent trials used in each case is 10^4. It is shown that the results obtained by using the analytical expression are in agreement with the MC results.

Inspection of these results in Fig. 2 highlights that the detection probability of the proposed detector decreases as the tunable parameter b increases in both the matched and mismatched cases. It

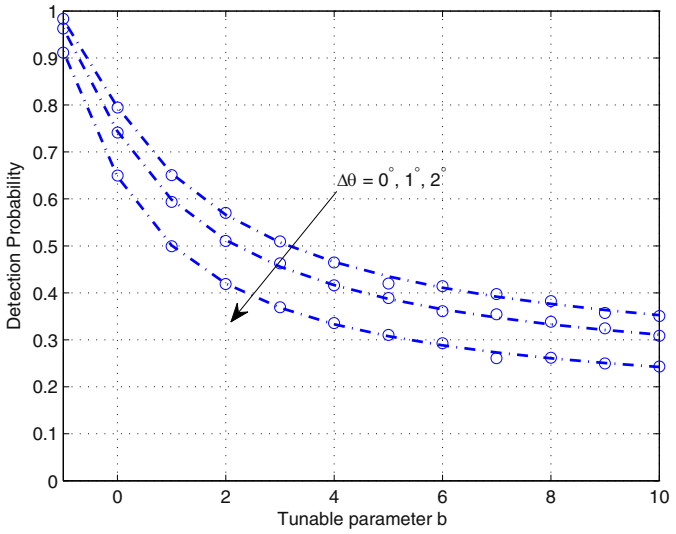

Fig. 2. Detection probability versus the tunable parameter b with $K = 16$ with the non-fluctuating target model. The lines denote the results obtained with the theoretical expression (26), while the symbols denote the MC results.

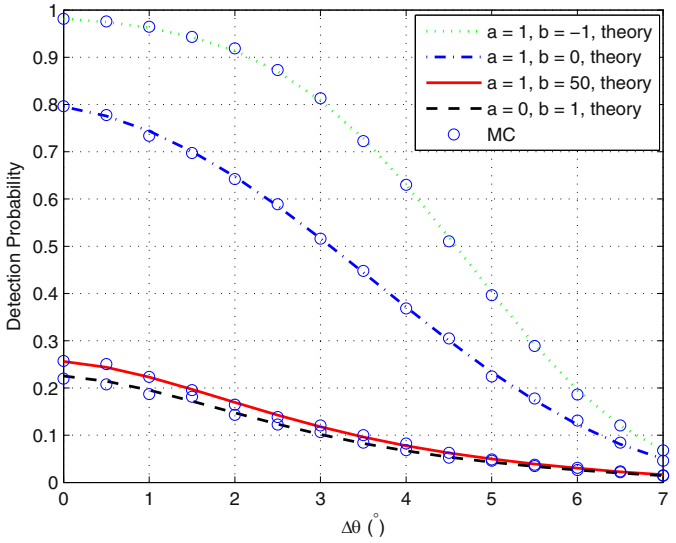

Fig. 3. Detection probability versus mismatched angle with SNR = 0 dB and $K = 16$ with the non-fluctuating target model. The lines denote the results obtained with the theoretical expression (26), while the symbols denote the MC results.

should be pointed out that the proposed detector with $a = 1$ and $b = -1$ has the same detection performance as Kelly's GLRT detector. However, the former has considerably lower computational burden than the latter, since the former only needs to calculate only one covariance estimator in the grid search stage.

In practice, we can choose the tunable parameters as $a = 1$ and $b = -1$ in order to achieve a high detection probability. However, a high detection probability is not always desired in the mismatched case (e.g., radar systems work in the target-tracking stage). As noted in [5], a detection is considered unsuccessful if the presence of target is declared while the beam is not aligned with the target direction. This is to say, the rejection capability of mismatched signal may be desired in the mismatched case.

In the next figure, the selective property of the proposed detector is illustrated for different tunable parameters. Fig. 3 presents the detection performance of the proposed detector as a function of the actual target direction θ, where the SNR is 0 dB and $K = 16$. It can be observed that for $a = 1$ the selective capability of the proposed detector increases as the tunable parameter b increases. When b is large enough (e.g., $b = 50$ in this example), the detector performs similarly to that with $a = 0$. This is because the parameter $a = 1$ can be neglected in the case of large b. Based on the above results in Figs. 2 and 3, we can select the minimal value $b = -1$ to achieve good detection performance for the matched signal, and choose a larger b to obtain stronger rejection capability of the mismatched signal. These numerical results highlight that the selectivity of the proposed detector can be flexibly adjusted.

It is worth noting that the selective capability is obtained at the cost of a loss in the detection performance in the matched case, which is shown in the following. In Fig. 4, the detection probability of the proposed detector as a function of SNR is demonstrated for different b and K with a non-fluctuating target. Here, we assume that no mismatch exists in the steering vector. We can observe that as the tunable parameter b increases, the detection performance of the proposed detector becomes worse. The performance gap between the case of $b = -1$ and the other cases is notable, especially when the training data size is limited (e.g., $K = 12$ in this example). This is due to the fact that target signal contamination significantly deteriorates the accuracy of the disturbance covariance matrix estimate obtained with limited training data. Note that the tunable detector with $b = -1$ is statistically equivalent to Kelly's GLRT detector, whose performance is not affected by target signal contamination. Nevertheless, it is shown in Fig. 4(c) that the effect of the signal contamination can be alleviated by using sufficient training data (e.g., $K = 24$ in this example). In addition, we can observe that a ceiling exists for the detection performance of the proposed detector with $b > -1$ in the case of limited training data. This is also caused by the target signal contamination in the estimate of the disturbance covariance matrix.

Fig. 5 depicts the detection performance of the proposed detector with a non-fluctuating target for the mismatched case where $\theta_0 = 11°$, i.e., $\Delta\theta = 1°$. The other parameters are the same as those in Fig. 4. We can see that the mismatch in the steering vector significantly degrades the detection performance. An interesting phenomenon observed is that the detection performance of the proposed detector with $b > -1$ is not a monotone function of the SNR in the mismatched case. In particular, the detection performance decreases dramatically in the region of high SNR. The observed phenomenon is consistent with that in [36,37]. This is because that the signal contamination with high SNR in the mismatched case significantly damages the accuracy in the disturbance covariance matrix estimate which is obtained by both the test and training data. For the case of $b = -1$, we have proved that the proposed detector in such a case is equivalent to Kelly's GLRT detector, as shown in Section 3. Therefore, the detection probability in this case does not decrease as the SNR increases.

In Fig. 6, we compare the detection performance of the proposed detector in the presence of a fluctuating target with different Q. Here we select $K = 16$ and define $\mathrm{SNR} = 10\log_{10}\frac{\sigma_\alpha^2}{\sigma_n^2}$. One can observe that as Q decreases, the detection performance improves in the low SNR region (e.g., SNR $\in [-20, -10]$ dB in this example), but decreases in the high SNR region. This phenomenon can be explained as follows. The depth of the amplitude fluctuation is ruled by the scale parameter Q. The lower the scale parameter Q, the wider the fluctuation span. Wide fluctuation spans can result in a gain in the detection performance for a low SNR, but lead to a loss in the detection performance for a high SNR.

The mismatched case with a fluctuating target is examined in Fig. 7, where $\Delta\theta = 1°$. It is shown that in the mismatched case the detection performance of the proposed detector is not a monotone function with respect to the SNR. This observation with the fluctuating model is similar to that made for the non-fluctuating model in Fig. 5.

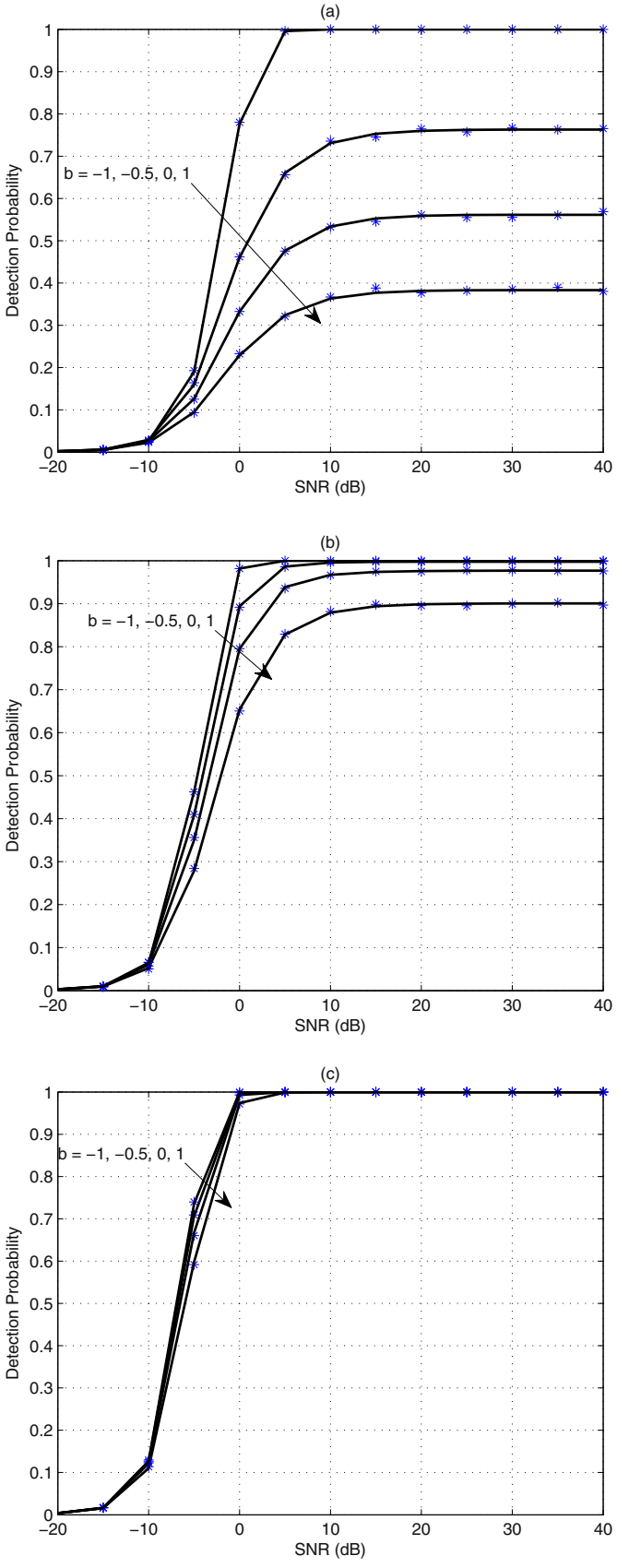

Fig. 4. Detection probability versus SNR with different b for the matched case with the unfluctuating target model. The lines denote the results obtained with the theoretical expression (26), while the symbols denote the MC results. (a) $K = 12$; (b) $K = 16$; (c) $K = 24$.

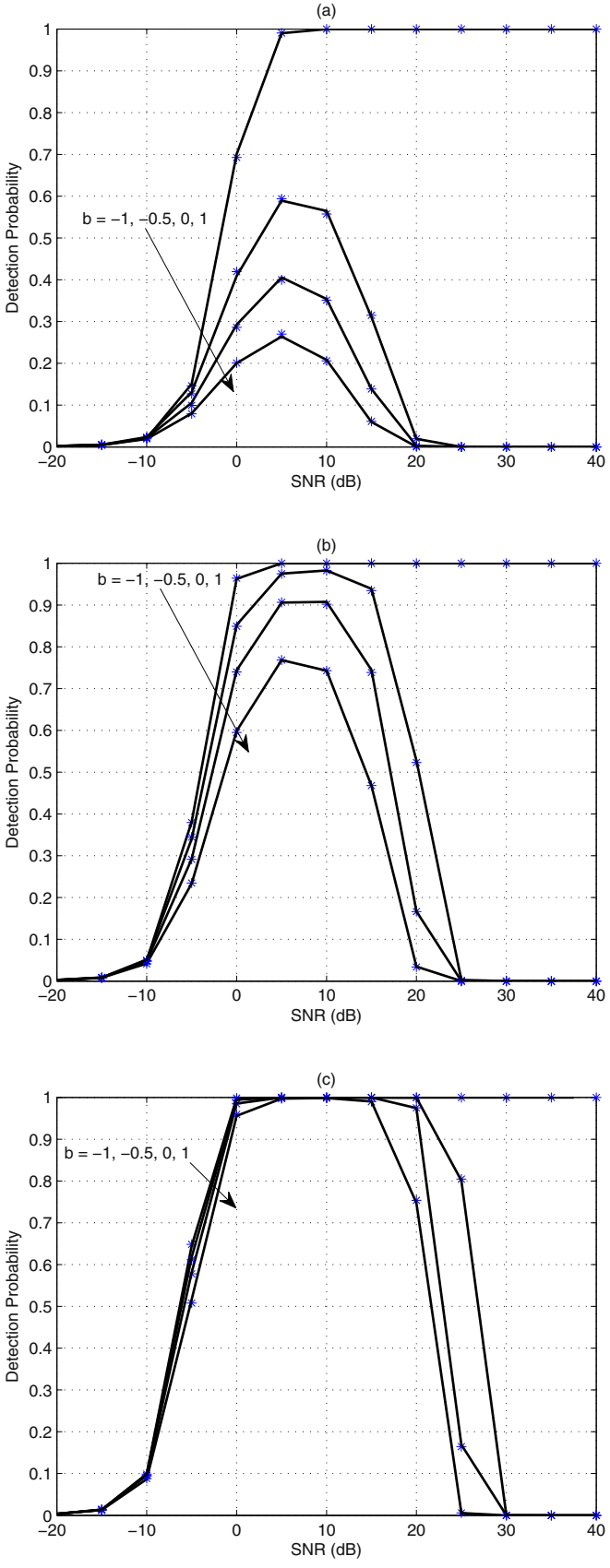

Fig. 5. Detection probability versus SNR with different b for the mismatched case with the non-fluctuating target model. The lines denote the results obtained with the theoretical expression (26), while the symbols denote the MC results. (a) $K = 12$; (b) $K = 16$; (c) $K = 24$.

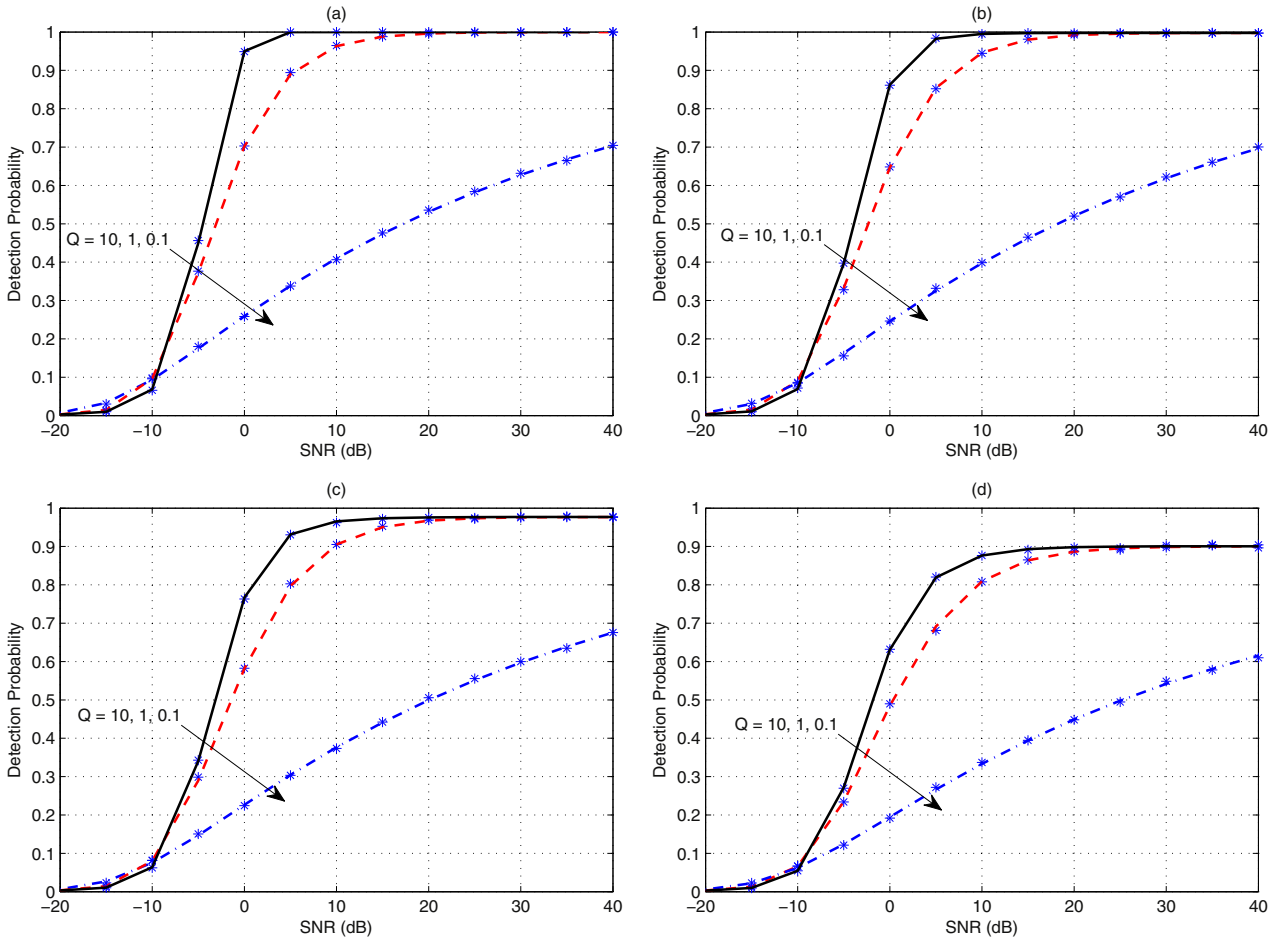

Fig. 6. Detection probability versus SNR with different Q for the matched case with the fluctuating model. The lines denote the results obtained with the theoretical expression (34), while the symbols denote the MC results. (a) $b=-1$; (b) $b=-0.5$; (c) $b=0$; (d) $b=1$.

5. Conclusion

We investigated the adaptive detection problem in colored Gaussian disturbance with an unknown covariance matrix. Both the test and training data are used to form an estimate of the disturbance covariance matrix. This scheme is considerably less complex to implement than the conventional ML estimate which only uses the training data. Based on the new estimator, we proposed a detector with two tunable parameters a and b. In particular, the proposed detector with $a=1$ and $b=-1$ has the same detection performance as Kelly's GLRT detector, but has a much lower computational burden. The statistical properties of the proposed detector were investigated in the general case where the practical target steering vector may not be aligned with the nominal one. Closed-form expressions for the probability of false alarm and the probability of detection of the proposed detector was derived for both unfluctuating and fluctuating target models. It is indicated that the proposed detector has the CFAR against the disturbance covariance matrix. The mismatched signal rejection capability of the proposed detector can be flexibly adjusted. More specifically, this selective property of the proposed detector can be improved by increasing the value of b (with fixed a).

Acknowledgments

This work was supported by National Natural Science Foundation of China under Contracts 61501351 and 61501505, and the National Science Fund for Distinguished Young Scholars under Grant 61525105.

Appendix A. Equivalent transformation of Λ

Applying the Sherman–Morrison–Woodbury formula [38] to (7), we have

$$\tilde{\mathbf{R}}^{-1}=\hat{\mathbf{R}}^{-1}-\frac{\hat{\mathbf{R}}^{-1}\mathbf{x}\mathbf{x}^{\dagger}\hat{\mathbf{R}}^{-1}}{1+\mathbf{x}^{\dagger}\hat{\mathbf{R}}^{-1}\mathbf{x}}. \tag{41}$$

As a result,

$$\mathbf{s}^{\dagger}\tilde{\mathbf{R}}^{-1}\mathbf{s}=\mathbf{s}^{\dagger}\hat{\mathbf{R}}^{-1}\mathbf{s}-\frac{|\mathbf{s}^{\dagger}\hat{\mathbf{R}}^{-1}\mathbf{x}|^{2}}{1+\mathbf{x}^{\dagger}\hat{\mathbf{R}}^{-1}\mathbf{x}}, \tag{42}$$

$$\mathbf{s}^{\dagger}\tilde{\mathbf{R}}^{-1}\mathbf{x}=\frac{\mathbf{s}^{\dagger}\hat{\mathbf{R}}^{-1}\mathbf{x}}{1+\mathbf{x}^{\dagger}\hat{\mathbf{R}}^{-1}\mathbf{x}}, \tag{43}$$

and

$$\mathbf{x}^{\dagger}\tilde{\mathbf{R}}^{-1}\mathbf{x}=\frac{\mathbf{x}^{\dagger}\hat{\mathbf{R}}^{-1}\mathbf{x}}{1+\mathbf{x}^{\dagger}\hat{\mathbf{R}}^{-1}\mathbf{x}}. \tag{44}$$

Substituting (42)–(44) into (8), and after some algebra, we obtain

$$\begin{aligned}\Lambda&=\frac{\frac{|\mathbf{s}^{\dagger}\hat{\mathbf{R}}^{-1}\mathbf{x}|^{2}}{(1+\mathbf{x}^{\dagger}\hat{\mathbf{R}}^{-1}\mathbf{x})(\mathbf{s}^{\dagger}\hat{\mathbf{R}}^{-1}\mathbf{s})}}{\left[1-\frac{|\mathbf{s}^{\dagger}\hat{\mathbf{R}}^{-1}\mathbf{x}|^{2}}{(1+\mathbf{x}^{\dagger}\hat{\mathbf{R}}^{-1}\mathbf{x})(\mathbf{s}^{\dagger}\hat{\mathbf{R}}^{-1}\mathbf{s})}\right]\left[a+(a+b)\mathbf{x}^{\dagger}\hat{\mathbf{R}}^{-1}\mathbf{x}\right]}\\&=\frac{T_{\mathrm{GLRT}}}{[1-T_{\mathrm{GLRT}}]\left[a+(a+b)\mathbf{x}^{\dagger}\hat{\mathbf{R}}^{-1}\mathbf{x}\right]}.\end{aligned} \tag{45}$$

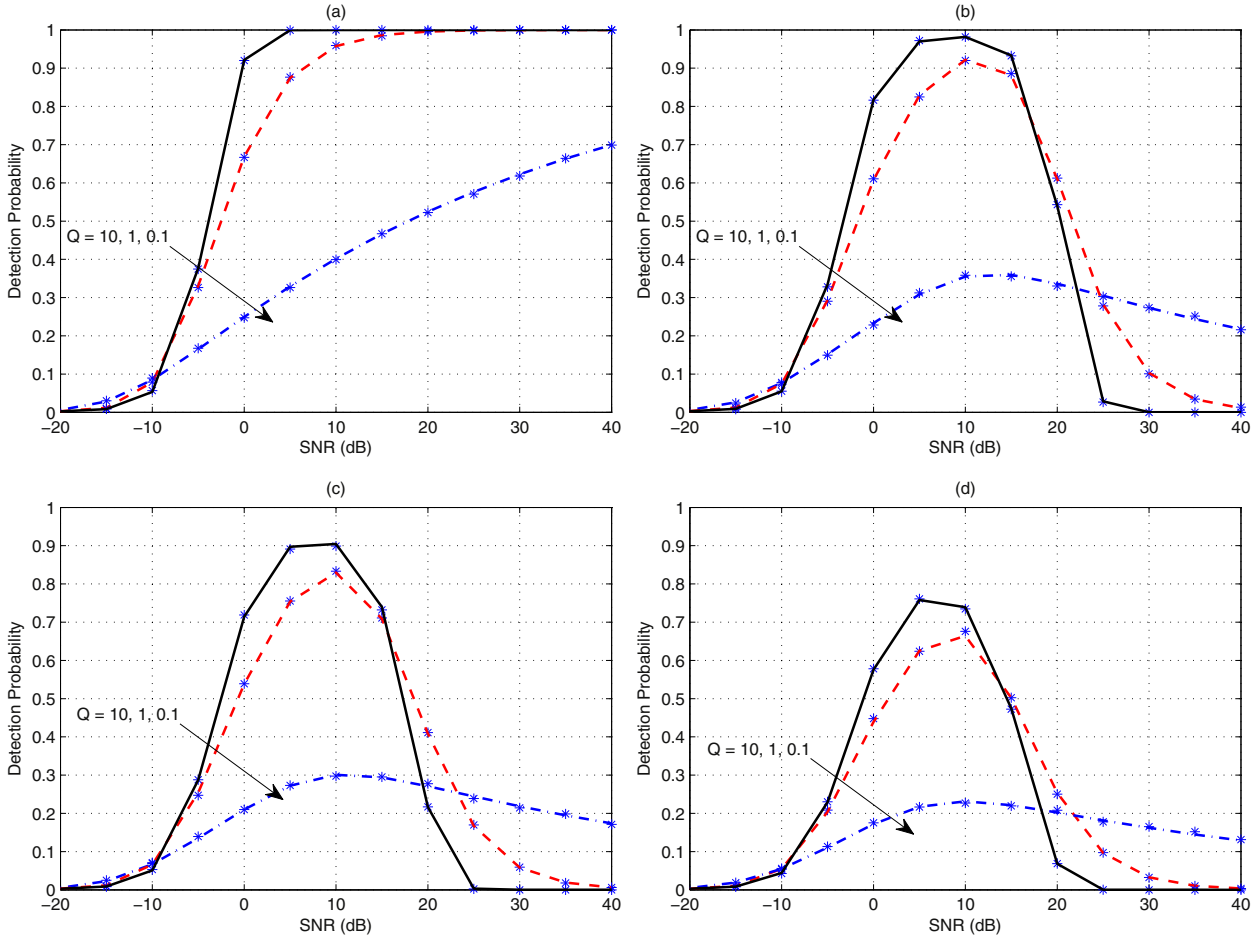

Fig. 7. Detection probability versus SNR with different Q for the mismatched case with the fluctuating model. The lines denote the results obtained with the theoretical expression (34), while the symbols denote the MC results. (a) $b=-1$; (b) $b=-0.5$; (c) $b=0$; (d) $b=1$.

Obviously, when $a=1$ and $b=-1$, the decision statistic Λ in (45) is equivalent to the Kelly's GLRT in [1]. According to (4) and (5), we have

$$\mathbf{x}^{\dagger}\hat{\mathbf{R}}^{-1}\mathbf{x}=\frac{T_{\mathrm{AMF}}}{T_{\mathrm{GLRT}}}-1. \tag{46}$$

Taking (4) and (46) into (45) leads to

$$\Lambda=\frac{T_{\mathrm{GLRT}}^{2}}{(1-T_{\mathrm{GLRT}})[(a+b)\,T_{\mathrm{AMF}}-b\,T_{\mathrm{GLRT}}]}. \tag{47}$$

From (10) and (11), we have

$$T_{\mathrm{GLRT}}=\frac{\bar{T}_{\mathrm{GLRT}}}{1+\bar{T}_{\mathrm{GLRT}}}, \tag{48}$$

and

$$T_{\mathrm{AMF}}=\frac{\bar{T}_{\mathrm{GLRT}}}{\rho}. \tag{49}$$

Inserting (48) and (49) into (47) yields

$$\begin{aligned}\Lambda&=\frac{\frac{\bar{T}_{\mathrm{GLRT}}^{2}}{(1+\bar{T}_{\mathrm{GLRT}})^{2}}}{\frac{1}{1+\bar{T}_{\mathrm{GLRT}}}\left[(a+b)\frac{\bar{T}_{\mathrm{GLRT}}}{\rho}-b\frac{\bar{T}_{\mathrm{GLRT}}}{1+\bar{T}_{\mathrm{GLRT}}}\right]}\\&=\frac{\rho\bar{T}_{\mathrm{GLRT}}}{(a+b)(1+\bar{T}_{\mathrm{GLRT}})-b\rho}\underset{H_0}{\overset{H_1}{\gtrless}}\lambda.\end{aligned} \tag{50}$$

After an equivalent transformation, we can obtain (12).

References

[1] E.J. Kelly, An adaptive detection algorithm, IEEE Trans. Aerosp. Electron. Syst. 22 (1) (1986) 115–127.

[2] E.J. Kelly, K. Forsythe, in: Adaptive Detection and Parameter Estimation for Multidimensional Signal Models, Lincoln Laboratory, MIT, 1989. Technical Report 848

[3] F.C. Robey, D.R. Fuhrmann, E.J. Kelly, R. Nitzberg, A CFAR adaptive matched filter detector, IEEE Trans. Aerosp. Electron. Syst. 28 (1) (1992) 208–216.

[4] S. Kraut, L.L. Scharf, R.W. Butler, The adaptive coherence estimator: A uniformly-most-powerful-invariant adaptive detection statistic, IEEE Trans. Signal Process. 53 (2) (2005) 417–438.

[5] N.B. Pulsone, C.M. Rader, Adaptive beamformer orthogonal rejection test, IEEE Trans. Signal Process. 49 (3) (2001) 521–529.

[6] A. De Maio, G. Ricci, A polarimetric adaptive matched filter, Signal Process. 81 (12) (2001) 2583–2589.

[7] F. Bandiera, D. Orlando, G. Ricci, CFAR detection of extended and multiple point-like targets without assignment of secondary data, IEEE Signal Process. Lett. 13 (4) (2006) 240–243.

[8] A. De Maio, Rao test for adaptive detection in Gaussian interference with unknown covariance matrix, IEEE Trans. Signal Process. 55 (7) (2007) 3577–3584.

[9] F. Bandiera, A. De Maio, G. Ricci, Adaptive CFAR radar detection with conic rejection, IEEE Trans. Signal Process. 55 (6) (2007) 2533–2541.

[10] F. Bandiera, D. Orlando, G. Ricci, Advamced Radar Detection Schemes Under Mismatched Signal Models, Morgan & Claypool, 2009.

[11] Q. He, N.H. Lehmann, R.S. Blum, A.M. Haimovich, MIMO radar moving target detection in homogeneous clutter, IEEE Trans. Aerosp. Electron. Syst. 46 (3) (2010) 1290–1301.

[12] A. De Maio, A. Farina, G. Foglia, Knowledge-aided Bayesian radar detectors & their application to live data, IEEE Trans. Aerosp. Electron. Syst. 46 (1) (2010) 170–183.

[13] C. Hao, D. Orlando, X. Ma, C. Hou, Persymmetric Rao and Wald tests for partially homogeneous environment, IEEE Signal Process. Lett. 19 (9) (2012) 587–590.

[14] A. Aubry, A. De Maio, L. Pallotta, A. Farina, Radar detection of distributed targets in homogeneous interference whose inverse covariance structure is defined via unitary invariant functions, IEEE Trans. Signal Process. 61 (20) (2013) 4949–4961.
[15] S. Lei, Z. Zhao, Z. Nie, Q.-H. Liu, A CFAR adaptive subspace detector based on a single observation in system-dependent clutter background, IEEE Trans. Signal Process. 62 (20) (2014) 5260–5269.
[16] C. Hao, D. Orlando, G. Foglia, X. Ma, S. Yan, C. Hou, Persymmetric adaptive detection of distributed targets in partially-homogeneous environment, Digital Signal Process. 24 (2014) 42–51.
[17] S. Lei, Z. Zhao, Z. Nie, Q.-H. Liu, Adaptive polarimetric detection method for target in partially homogeneous background, Signal Process. 106 (2015) 301–311.
[18] M.S. Greco, A. De Maio, Modern Radar Detection Theory, IET, 2015.
[19] A. Aubry, A. De Maio, G. Foglia, D. Orlando, Diffuse multipath exploitation for adaptive radar detection, IEEE Trans. Signal Process. 63 (5) (2015) 1268–1281.
[20] N.B. Pulsone, M.A. Zatman, A computationally efficient two-step implementation of the GLRT, IEEE Trans. Signal Process. 48 (3) (2000) 609–616.
[21] F. Bandiera, D. Orlando, G. Ricci, One- and two-stage tunable receivers*, IEEE Trans. Signal Process. 57 (8) (2009) 3264–3273.
[22] F. Bandiera, D. Orlando, G. Ricci, A subspace-based adaptive sidelobe blanker, IEEE Trans. Signal Process. 56 (9) (2008a) 4141–4151.
[23] F. Bandiera, O. Besson, D. Orlando, G. Ricci, An improved adaptive sidelobe blanker, IEEE Trans. Signal Process. 56 (9) (2008b) 4152–4161.
[24] J. Ward, Space-Time Adaptive Processing for Airborne Radar, Technical Report 1015, Lincoln Laboratory, MIT, December 1994.
[25] A. Cameron, The jindalee operational radar network: Its architecture and surveillance capability, in: Proceedings of IEEE Radar, 1995, pp. 692–697.
[26] K. Gerlach, A comparison of two adaptive detection schemes, IEEE Trans. Aerosp. Electron. Syst. 30 (1) (1994) 30–40.
[27] B.O. Steenson, Detection performance of a mean-level threshold, IEEE Trans. Aerosp. Electron. Syst. (4) (1968) 529–534.
[28] G.M. Dillard, Mean-level detection of non uctuating signals, IEEE Trans. Aerosp. Electron. Syst. (6) (1974) 795–799.
[29] E.J. Kelly, Adaptive Detection in Nonstationary Interference–Part III, Technical Report 761, Lincoln Laboratory, MIT, 1987.
[30] J. Liu, Z.-J. Zhang, Y. Yang, H. Liu, A CFAR adaptive subspace detector for first-order or second-order Gaussian signals based on a single observation, IEEE Trans. Signal Process. 59 (11) (2011) 5126–5140.
[31] I.S. Gradshteyn, I.M. Ryzhik, Table of Integrals, Series, and Products, seventh, Academic Press, San Diego, 2007.
[32] A. De Maio, A. Farina, G. Foglia, Target fluctuation models and their application to radar performance prediction, IEE Proc. Radar Sonar Navig. 151 (5) (2004) 261–269.
[33] A. De Maio, Robust adaptive radar detection in the presence of steering vector mismatches, IEEE Trans. Aerosp. Electron. Syst. 41 (4) (2005) 1322–1337.
[34] G. Cui, A. De Maio, M. Piezzo, Performance prediction of the incoherent radar detector for correlated generalized Swerling-Chi fluctuating targets, IEEE Trans. Aerosp. Electron. Syst. 49 (1) (2013) 356–368.
[35] G. Cui, A. De Maio, A. Aubry, A. Farina, L. Kong, Advanced SLB architectures with invariant receivers, IEEE Trans. Aerosp. Electron. Syst. 49 (2) (2013) 798–818.
[36] K.J. Sohn, H. Li, B. Himed, Parametric GLRT for multichannel adaptive signal detection, IEEE Trans. Signal Process. 55 (11) (2007) 5351–5360.
[37] D. Sengupta, S.M. Kay, Parameter estimation and GLRT detection in colored non-Gaussian autoregressive processes, IEEE Trans. Acoust. Speech Signal Process. 38 (10) (1990) 1661–1676.
[38] M. Woodbury, Inverting Modified Matrices, Memorandum Report 42, Statistical Research group, Princeton, 1950.